Iranian Journal of Oil & Gas Science and Technology, Vol. 4 (2015), No. 1, pp. 81-91
http://ijogst.put.ac.ir

An Electrochemical Investigation of Nano Cerium Oxide/Graphene as an Electrode Material for Supercapacitors

Mohammadreza Shishesaz[1*], Mehdi Robat Sarpoushi[1], and Mohammad Ali Golozar[2]

[1] Technical Inspection Engineering Department, Petroleum University of Technology, Abadan, Iran
[2] Materials Science Engineering Department, Isfahan University of Technology, Isfahan, Iran

Received: August 07, 2013; revised: October 04, 2013; accepted: May 20, 2014

Abstract

In this paper, the effect of cationic and anionic ion sizes on the charge storage capability of graphene nanosheets is investigated. The electrochemical properties of the produced electrode are studied using cyclic voltammetry (CV) and electrochemical impedance spectroscopy (EIS) techniques in 3M NaCl, NaOH, and KOH electrolytes. Scanning electron microscopy (SEM) is used to characterize the microstructure and nature of the prepared electrode. The SEM images and X-ray diffraction (XRD) patterns confirm the layered structure (12 nm thickness) of the used graphene with an interlayer distance of 3.36 Å. The electrochemical results and the ratio of q_o^*/q_T^* confirm good charge storage and charge delivering capability of the prepared electrode in the 3M NaCl electrolyte. Charge/discharge cycling tests show a good reversibility and confirm that the solution resistance will increase after 500 cycles.

Keywords: Electronic Materials, Nanostructures, Electrochemical Measurement, Electrical Properties, Energy Storage

1. Introduction

Recently, electrochemical capacitors have attracted worldwide research interests. Depending on charge storage mechanisms, capacitors can be classified in three types: electrochemical double layer capacitors (EDLC's), faradic pseudocapacitors and hybrid capacitors (Conway, 1999; Conway, 2002; Hadjipaschalis et al., 2009; Zhang et al., 2009). Especially in EDLC's and at high charge/discharge rates, since no chemical action is involved, the effects are easily reversible with a minimal degradation in deep discharge or overcharge and typical life cycle is hundreds of thousands of cycles (Yan et al., 2010; Soldano et al., 2010; Singh et al., 2011). With respect to the electrode materials, there are three main categories, namely carbon-based materials, transition metal oxides, and conductive polymers (Nasibi et al., 2013; Babakhani et al., 2011). Among carbon-based materials, due to the good conductivity, superior chemical stability, a large surface-to-volume ratio, and its unique layered structure, graphene has competed with carbon nanotubes, activated carbon, etc., which have been used as the electrode material for EC's. The high surface area of graphene does not depend on the distribution of pores in solid state, but comes from the interconnected open channels between graphene layers distributed in a two-dimensional architecture (Burke, 2000; Ardizzone et al., 2000;

* Corresponding Author:
Email: shishesaz@put.ac.ir

Yoshio et al., 2006; Honda et al., 2007). However, the major problem of such a material is that not all the BET surface area is electrochemically accessible (Kim et al., 2006). Ion sizes in the electrolyte and the charge/discharge rate are of significant parameters affecting the ratio of accessible to the total surface, the energy storage, and power capability of the graphene electrode. Therefore, choosing a proper electrolyte in accordance with the morphology may be affective.

In this paper, the effect of ion size on charge storage, charge delivering capability, and the reversibility of graphene electrodes were investigated using cyclic voltammetry and electrochemical impedance spectroscopy techniques. The morphology and the nature of the prepared electrodes were investigated employing scanning electron microscopy.

2. Experimental

2.1. Materials

Graphene nanopowder (60 nm multi-layered flakes) with a purity of 98.5% was purchased from graphene supermarket and polytetrafluoroethylene (<2 μm) was supplied by Aldrich company. All the other chemicals used in this study were purchased from Merck. 90 wt.% graphene nanopowder and 10 wt.% polytetrafluoroethylene (PTFE) were well mixed by ultrasonic wave in ethanol in a paste form for about 60 min. The paste form was chosen for a better dispersion of PTFE in graphene nanoflakes. After drying the paste and powdering, the composite was pressed onto a 316-l stainless steel plate (5×10^7 Pa), which served as a current collector (surface area was 1.22 cm^2). A steel rod and hollow cylinder of epoxy was used for pressing. The composite was pressed into the epoxy cylinder properly by the steel rod. Teflon paper was used at the bottom of the rod because of very low adhesion in order for the composite material not to stick to the stainless steel substrate. The typical mass load of the electrode material was 45 mg. The electrolytes investigated were 3 M NaCl, NaOH, and KOH.

3. Characterization

The electrochemical behavior of the prepared electrodes was characterized using CV and EIS tests. The electrochemical measurements were performed using an Autolab (Netherlands) Model PGSTAT302N. The CV tests were performed within the range of -0.55 to +0.3 V (vs. SCE). The EIS measurements were carried out in the frequency range of 100 kHz to 0.02 Hz at OCP with an AC amplitude of 10 mV. The specific capacitance C (Fg^{-1}) of the active material was determined by integrating either the oxidative or reductive parts of the cyclic voltammogram curve (Q(C)). This charge was subsequently divided by the mass of the active material m (g) and the width of potential window of cyclic voltammogram ΔE (V), i.e., $C=Q/(m.\Delta V)$ (Fan et al., 2007; Wu et al., 2007; Yang et al., 2007).

4. Results and discussion

Specific surface area and conductivity are two important parameters to prepare highly efficient electrodes for capacitors. But, only a part of surface is always accessible by the electrolyte ions to be adsorbed. This would increase the solution resistance. Figure 1(a) shows the SEM image of the prepared electrodes confirming the 2D graphene nanosheets consisting of several carbon atom layers with a total thickness of about 12 nm. Graphene layers interact with each other to form open pore systems through which ions easily access the surfaces between the graphene nanosheets to form an electric double layer. The distance between these nanosheets was measured using XRD and was about 3.36 Å (Figure 1(b)). The used graphene was perpendicular to these nanosheets, showed no porosity, and was completely flat (Figure 1 (a)). Thus the used material is completely two-dimensionally

porous, while one-dimensionally flat. With this morphology, it seems that the charge storage depends directly on the charge separation on the flat part (which is the most accessible surface of the electrode) and on open pore systems (which are less accessible and ion-size dependant) simultaneously. Ion sizes and ion diffusion through these pores would affect the activation of these less accessible surfaces, especially at high scan rates (Lao et al., 2006). Increasing the ionic radius would decrease the number of adsorbed ions on the unit surface area of the electrode. This would decrease the stored charge on the outer Helmholtz layer. Therefore, for further investigations, the 3M electrolytes of KOH, NaOH, and NaCl were employed. The main difference of these electrolytes is the effective radius of their anions and cations. Na^+, K^+, Cl^-, and OH^- ions have effective radiuses of 102, 138, 181, and 153 (pm) respectively. The ratio of interlayer distance of graphene 3.36 Å to ionic radius (α) for these ions would be 3.29, 2.43, 1.86, and 2.20 respectively.

The capacitance of each electrode was calculated from the CV curves using Equation 1:

$$C_s = \int idV \, \frac{\Delta V}{ms} \tag{1}$$

where, C_s is the specific capacitance and $\int idV$ is the integrated area of the CV curve; m represents the mass of active material (mass of the electrode material regardless of the mass of PTFE). ΔV and s stand for the potential range and the scan rate respectively.

Figure 1(c) shows the first cyclic voltammetry curves of the prepared electrodes at the scan rate of 100 mVs^{-1} in different electrolytes. All the CV's exhibit a rectangular shaped profile which is a good characteristic of an ideal capacitive behavior. All of the electrode/electrolyte systems exhibited almost potential independent double layer capacitance. The prepared electrodes showed a low current density in 3M KOH electrolyte, while it increased in 3M NaOH and NaCl electrolytes (Figure 1(c)). Increasing the ionic radius could decrease the ionic diffusion through the pores and cause a lower current reversal at the final potentials (Figure 1(c)). Table 1 represents capacitance at a scan rate of 100 mV/s in all the three electrolytes. NaCl solution possessed the maximum capacitance among these electrolytes. The point of intersecting the Nyquist curves with the real axis in the range of high frequency shows the equivalent series resistance (ESR) (Figure 1(d)). It indicates the total resistance of the electrode, the bulk electrolyte resistance, and the resistance at the electrolyte/electrode interface (Zhao et al., 2007; Okajima et al., 2005; Xing et al., 2006; Choi et al., 2006).Therefore, two counter-acting parameters would act simultaneously as the ionic radius increases, namely increasing the electrical resistance and decreasing the charge adsorption on the surface of the prepared electrodes. In order to obtain quantitative information on the utilization of the prepared graphene electrodes, the voltammograms were analyzed as a function of scan rate using the procedure reported by Ardizzone et al. (Katakabe et al., 2005; Barbieri et al., 2005). Figures 2a, 2b, and 2c exhibit the cyclic voltammetry curves obtained using different scan rates in 3M KOH, NaOH, and NaCl electrolytes. Table 2 represents capacitance at different scan rates in NaCl solution (the optimum solution). In charge and discharge cycles, the total charge can be written as the sum of an inner charge from the less and an outer charge from the more accessible reaction sites, i.e., $q_T^* = q_I^* + q_O^*$; where, q_T^*, q_I^*, and q_O^* are the total charge, and charges related to the inner surface, and charges related to the outer surface respectively (Danaee et al., 2009; Kotz et al., 2000). The extrapolation of q^* to s=0 in $1/q^*$ vs. $s^{1/2}$ plot (Figure 2(d)) gives total charge q_T^* which is the charge related to the entire active surface of the electrode. In addition, the extrapolation of q^* to s=∞ ($s^{-1/2}$ = 0) in q^* vs. $s^{-1/2}$ plot (Figure

2(e)) gives the outer charge q_O^*, which is charge on the most accessible active surface. The prepared electrode show the ratio of the outer to the total charge ($\frac{q_O^*}{q_T^*}$) of 0.077 in the NaCl electrolyte.

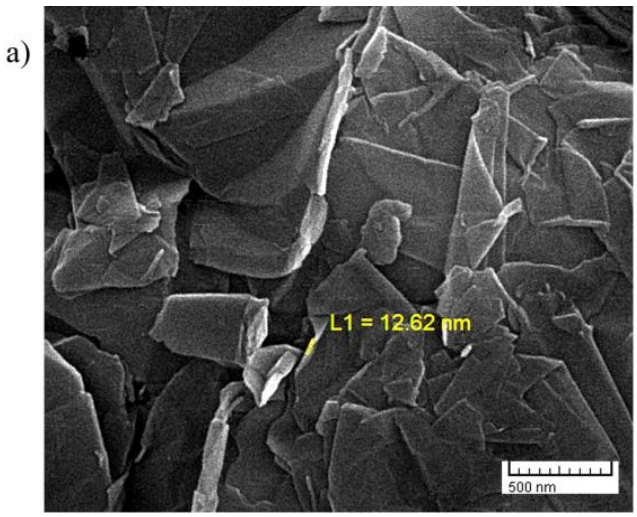

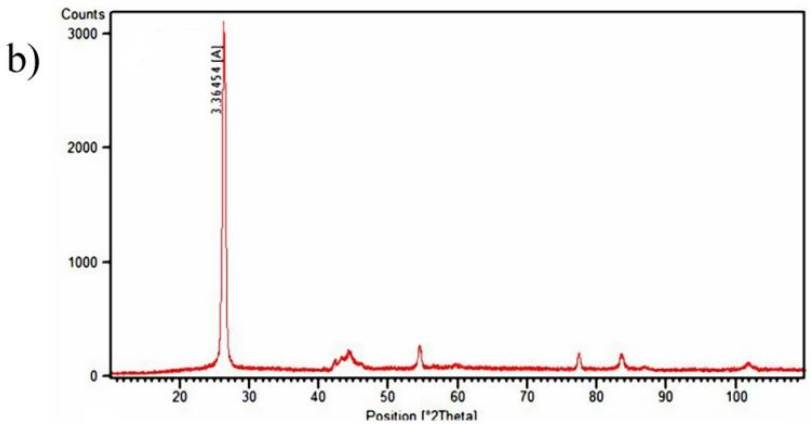

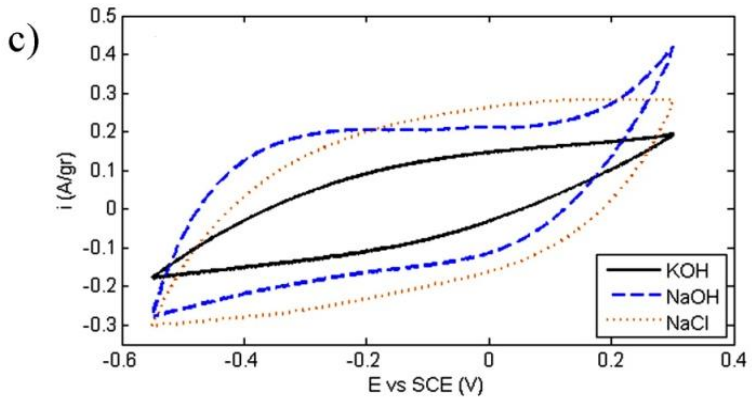

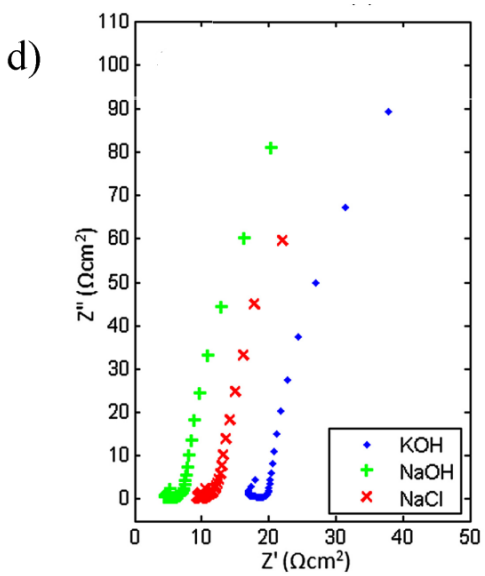

Figure 1
(a) Scanning electron microscopy image; (b) the XRD pattern obtained from graphene electrode; (c) cyclic voltammetry curves; and (d) Nyquist diagrams obtained from graphene electrode in different electrolytes.

Table 1
Capacitance (100mV/s) in different electrolytes.

Electrolyte	Capacitance (100mV/s)
NaCl	1.99 F/gr
KOH	1.09 F/gr
NaOH	1.84 F/gr

Table 2
Capacitance at different scan rates in NaCl solution.

Scan Rate	Capacitance
5 mV/s	3.62 F/gr
30 mV/s	2.67 F/gr
50 mV/s	2.38 F/gr
100 mV/s	1.99 F/gr
200 mV/s	1.40 F/gr
300 mV/s	1.05 F/gr
500 mV/s	0.71 F/gr

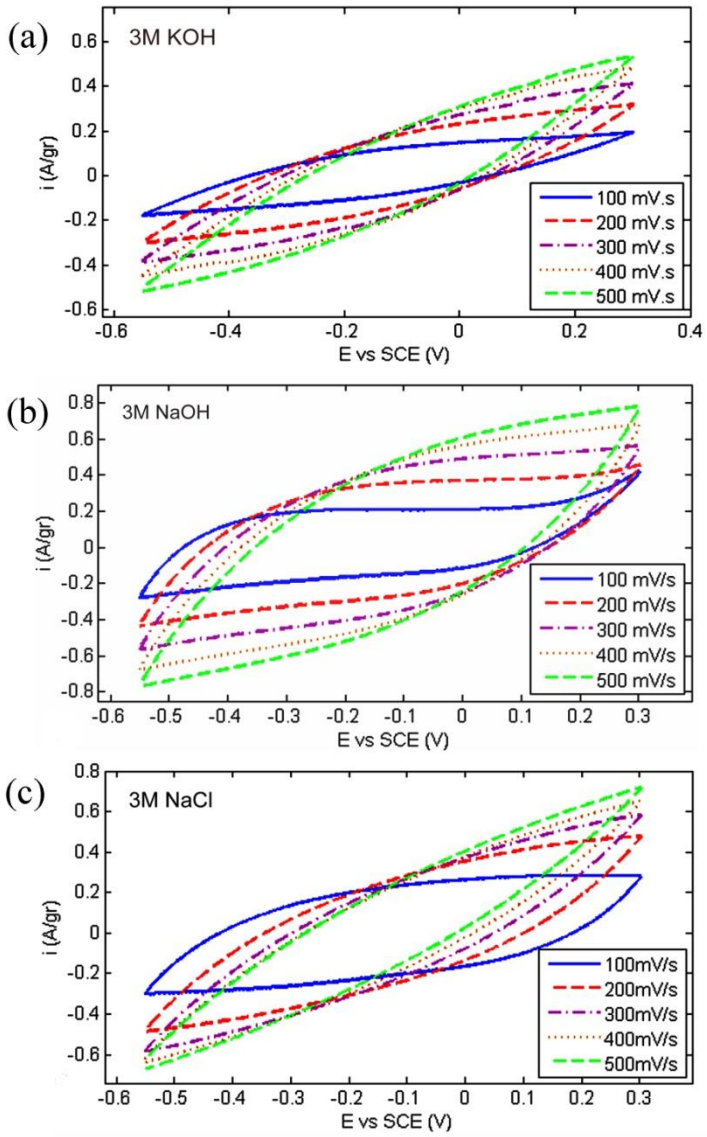

Figure 2
Cyclic voltammetry curves obtained using different scan rates in 3M (a) KOH, (b) NaOH, and (c) NaCl electrolytes; (d) The extrapolation of q to s=0 in the $(q^*)^{-1}$ vs. $s^{0.5}$ plot giving the total charge; and (e) extrapolation of q to s=∞ in the q vs. $s^{-0.5}$ plot giving the outer charge for the graphene electrode in NaCl electrolyte.

As the scan rate increases (Figure 3(a)), the capacitance versus potential relation would deviate from the classical square waveform, which is expected for a pure capacitor. As discussed by some researchers, this is due to the resistance effects down the pores (Singh et al., 2011). Additionally, efficiency is another important parameter affecting the capacitance at high sweep rates. As the sweep rate increases, the loss of energy rises and the stored charge on the electrode surface drops; this causes the capacitance efficiency to decrease (Figure 3(a)). The graphene electrode shows a low capacitance of 3.62 Fg^{-1} in the 3M NaCl electrolyte. It seems that the low ionic diffusion due to low interlayer distances, which is a unique property of the graphene nanosheets, may be the main reason for this low capacitance.

Regarding the practical applications, the cycle stability of supercapacitors is a crucial parameter. The cycle lives of both conducting polymers and metal oxides, as candidates for pseudocapacitive materials, are much shorter than those of the carbon-based materials because of the loss of active materials. In the case of graphene nanosheets, the cycle stability was evaluated by repeating the CV at a scan rate of 100 mVs^{-1} for 500 cycles (Figure 3(b)). Simultaneously, the EIS tests were used to evaluate the electrode changes (Figure 3(c)). Graphene was found to exhibit excellent stability over the entire cycle numbers (Figure 3(b)). The anodic and cathodic currents decreased, but the cyclic voltammetry curves remained in their rectangular shaped profiles (Figure 3(b)). Conversely, the charge stored on the electrode decreased only by ~23% of the initial charge stored on the electrode (Table 3). These behaviors demonstrate a good cycling stability. Most capacitors, except for the vacuum or air types, do not exhibit ideal pure capacitive behavior according to the criterion that the real and imaginary components of their impedance should be out of phase by 90 ° independent of the frequency between the periodic changes of current and voltage when addressed by a sinusoidally alternating voltage. Most practical capacitors deviate from this requirement because their impedance is not that of a pure capacitance; it is, in fact, of a capacitance linked in series with an element exhibiting ohmic behavior, which in combination with the capacitance gives rise to a phase angle that is less than 90 ° and is usually frequency-dependent. This ohmic component is referred to as the equivalent series resistance (Conway, 1999). In all the three electrolytes, the phase angle is less than 90 °, because ESR is involved in all the three electrolytes. Figure 4 shows that the phase angle (φ) between E (voltage) and I (current) depends on the frequency in NaCl electrolyte. Equation 2 represents the relation between Z, E, and I:

$$Z = \frac{E_T}{I_T} = \frac{E_0 \sin(2\pi ft)}{I_0 \sin(2\pi ft + \varphi)} \quad = \frac{Z_0 \sin(2\pi ft)}{I_0 \sin(2\pi ft + \varphi)} \tag{2}$$

where, Z is the impedance and E_0 is the maximum voltage; I_0 stands for the maximum current, and f and t represent frequency and time respectively. One capacitive loop demonstrates only one reaction involved.

In this case, good coating as result of a proper applied pressure was one of the reasons for good cyclic stability. Although applying higher pressure may increase the cyclic stability due to the better adhesion of the coating on substrate, capacitance decreases dramatically. During the 500 charge/discharge cycles, the equivalent series resistance increased (Figure 3(c)) and Nyquist plots shifted to higher values, which can be attributed to the electrolyte decomposition on the electrode surface.

Table 3
Capacitance over the 500 cycles in NaCl solution.

Cycle Number	Capacitance (100mV/s)
1 Cycle	1.99 F/gr
50 Cycle	1.96 F/gr
200 Cycle	1.73 F/gr
500 Cycle	1.53 F/gr

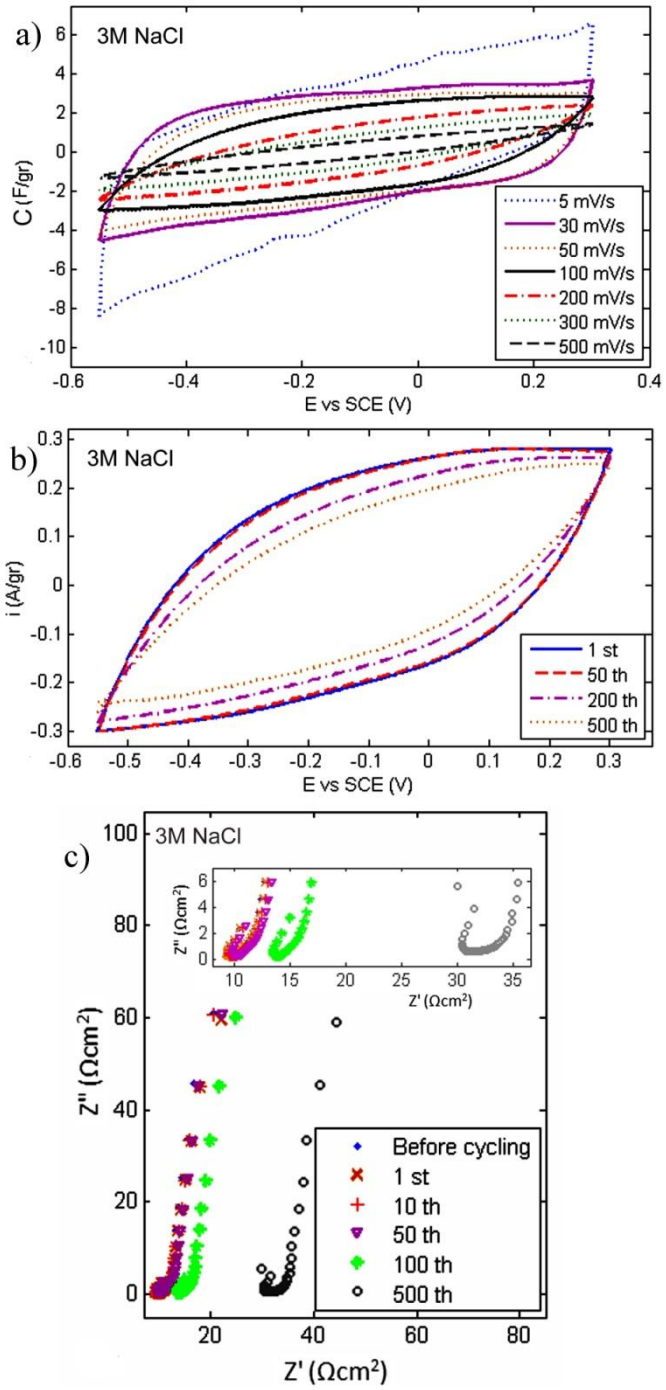

Figure 3

(a) Representative cyclic voltammograms obtained at different scan rates; (b) representative cyclic voltammetry obtained over 500 cycles; and (c) Nyquist plots after different cycles for graphene nanosheets in a 3M NaCl electrolyte.

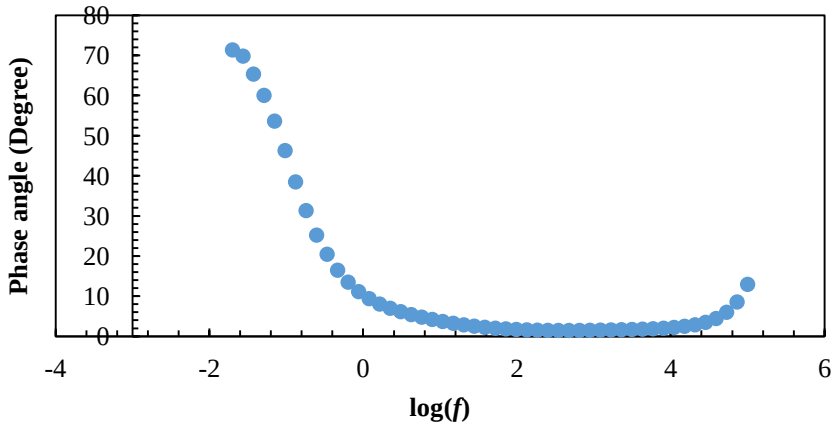

Figure 4
Bode plot (phase angle/degree vs. log (*f*)).

5. Conclusions

In summary, the studies confirmed the presence of flat and porous (having an interlayer distance of about 3.36 Å) surfaces and showed the dependency of energy storage and power capability of the used material on ion size and the charge/discharge rate. Good cycling performance was observed which was stemmed from a controlled thickness and subsequent changing of the substrate reactive states. A relatively high ratio of $\frac{q_o^*}{q_T^*}$ (0.077) confirmed the high current response on voltage reversal in a 3M NaCl electrolyte. The rectangular shaped profile, which is a good characteristic of an ideal capacitive behavior, was obvious over the entire cycle numbers. The charge stored on the electrode decreased only by ~23% of the initial charge stored on the electrode, which represented good reversibility. The proposed electrode provided a double layer capacitance and showed a capacitance of as high as 3.62 Fgr^{-1} at 5 mV s^{-1} in a 3M NaCl electrolyte.

Nomenclature

CV	: Cyclic voltammetry
EIS	: Electrochemical impedance spectroscopy
q_o^*	: Outer charge
q_T^*	: Total charge
SEM	: Scanning electron microscopy
XRD	: X-ray diffraction

References

Ardizzone, S., Fregonara, G., and Trasatti, S., Electrochim Acta, Vol. 35, p. 263-267, 2000.

Babakhani, B. and Ivey, D.G., Electrochim Acta, Vol. 56, p. 4753-4762, 2011.

Barbieri, O., Hahn, M., Herzog, A., and Kotz, R., Capacitance Limits of High Surface Area Activated Carbons for Double Layer Capacitors, Carbon,Vol. 43, p.1303–1310, 2005.

Burke, A., J. Power Sources, Vol. 91, p. 37–50, 2000.

Choi, D. and Kumta, PN., Nanocrystalline TiN Derived by a Two-step Halide Approach for Electrochemical Capacitors, Journal of Electrochemical Society, Vol. 153, p. 2298-2303, 2006.

Conway, B.E., Electrochemical Capacitors Scientific Fundamental and Technological Applications, New York, Kluwer Academic, Plenum, 1999.

Conway, B. E. and W.G. Pell, J. Power Sources, Vol. 105, p. 169–181, 2002.

Danaee, I., Jafarian, M., Forouzandeh, F., Gobal, F., and Mahjani, MG., Electrochemical Impedance Studies of Methanol Oxidation on GC/Ni and GC/NiCu Electrode, International Journal of Hydrogen Energy, Vol. 34, p. 859-869, 2009.

Fan, Z., Chen, J., Cui, K., Sun, F., Xu, Y., and Kuang, Y., Preparation and Capacitive Properties of Cobalt-nickel Oxides/Carbon Nanotube Composites, Electrochim Acta, Vol. 52, p. 2959-2965, 2007.

Hadjipaschalis, I., Poullikkas, A., and Efthimiou, V., Overview of Current and Future Energy Storage Technologies for Electric Power Applications, Renewable and Sustainable Energy Reviews, Vol. 13, p. 1513-1522, 2009.

Honda, Y., Haramoto, T., Takeshige, M., Shiozaki, H., Kitamura, T., and Ishikawa, M., Aligned MWCNT Sheet Electrodes Prepared by Transfer Methodology Providing High-power Capacitor Performance, Electrochem Solid-State Lett, Vol. 10, p. 106-110, 2007.

Katakabe, T., Kaneko, T., Watanabe, M., Fukushima, T., and Aida, T., Electric Double-layer Capacitors Using Bucky Gels Consisting of an Ionic Liquid and Carbon Nanotubes, Journal of Electrochemical Society, Vol. 152, p. 1913-1916, 2005.

Kim, I. H. and Kim, K. B., Electrochemical Characterization of Hydrous Ruthenium Oxide Thin-film Electrodes for Electrochemical Capacitor Applications, Journal of Electrochemical Society, Vol. 153, p. 383-389, 2006.

Kotz, R. and Carlen, M., Principles and Applications of Electrochemical Capacitors, Electrochimica Acta, Vol. 45, p. 2483-2498, 2000.

Lao, Z. J., Konstantinov, K., Tournaire, Y., Ng, SH., Wang, GX., and Liu, HK., Synthesis of Vanadium Pentoxide Powders with Enhanced Surface-area for Electrochemical Capacitors, Journal of Power Sources, Vol. 162, No. 2, p. 1451-1454, 2006.

Nasibi, M., Golozar, M.A., and Rashed, Gh., Nano Iron Oxide (Fe_2O_3)/Carbon Black Electrodes as Electrode Material for Electrochemical Capacitors: Effect of the Nanoparticles Dispersion Quality Materials Chemistry and Physics, Vol. 139, No. 1, p. 12-16, 2013.

Singh, V., Joung, D., Zhai, L., Das, S., Khondaker, S. A., and Seal, S., Graphene Based Materials: Past, Present and Future, Prog Mater SCI - Progress in Materials Science, Vol. 56, No. 8, p. 1178-1271, 2011.

Okajima, K., Ikeda, A., Kamoshita, K., and Sudoh, M., High Rate Performance of Highly Dispersed C60 on Activated Carbon Capacitor, Electrochim Acta, Vol. 51, No. 5, p. 972-977, 2005.

Soldano, C., Mahmood, A., and Dujardin, E., Production, Properties and Potential of Graphene Carbon, Vol. 48, No. 8, p. 2127-2150, 2010.

Wu, M. S., Huang, Y. A., Yang, C. H., and Jow, J. J., Electrodeposition of Nanoporous Nickel Oxide Film for Electrochemical Capacitors, International Journal of Hydrogen Energy, Vol. 32, No. 17, p. 4153-4159, 2007.

Xing, W., Qiao, SZ., Ding, RG., Li, F., Lu, GQ., Yan, ZF., and Cheng, H.M., Superior Electric Double Layer Capacitors Using Ordered Mesoporous Carbons, Carbon, Vol. 44, p. 216-224, 2006.

Yan, J., Wei, T., Shao, B., Ma, F., Fan, Zh., Zhanga, M., Zheng, Ch., Shang, Y., Qian, W., and Wei, F., Electrochemical Properties of Graphene Nanosheet/Carbon Black Composites as Electrodes for Supercapacitors, Carbon, Vol. 48, No. 6, p. 1731-1737, 2010.

Yang, X. H., Wang, Y. G., Xiong, H. M., and Xia, Y. Y., Interfacial Synthesis of Porous MnO_2 and its

Application in Electrochemical Capacitor, Electrochimica Acta, Vol. 53, No. 2, p. 752-757, 2007.

Zhang,Y., Feng, H., Wu, X., Wang, L., Zhang, A., Xia, T., Dong, H., Li, X., and Linsen Zhang, Progress of Electrochemical Capacitor Electrode Materials: A Review, International Journal of Hydrogen Energy, Vol. 34, No. 11, p. 4889-4899, 2009.

Zhao, D. D., Bao, S. J., Zhou, W. J., and Li, H. L., Preparation of Hexagonal Nanoporous Nickel Hydroxide Film and its Application for Electrochemical Capacitor, Electrochemistry Communications, Vol. 9, No. 5, p. 869-874, 2007.